Accepted for publication in ApJ
Preprint typeset using LaTeX style emulateapj v. 5/25/10

arXiv:1203.2925v1 [astro-ph.GA] 13 Mar 2012

TINY SCALE OPACITY FLUCTUATIONS FROM VLBA, MERLIN AND VLA OBSERVATIONS OF H I ABSORPTION TOWARD 3C 138

Nirupam Roy[1,2], Anthony H. Minter[3], W. M. Goss[1], Crystal L. Brogan[4] and T. J. W. Lazio[5]

Accepted for publication in ApJ

ABSTRACT

The structure function of opacity fluctuations is a useful statistical tool to study tiny scale structures of neutral hydrogen. Here we present high resolution observation of H I absorption towards 3C 138, and estimate the structure function of opacity fluctuations from the combined VLA, MERLIN and VLBA data. The angular scales probed in this work are $\sim 10-200$ milliarcsec (about $5-100$ AU). The structure function in this range is found to be well represented by a power law $S_\tau(x) \sim x^\beta$ with index $\beta \sim 0.33 \pm 0.07$ corresponding to a power spectrum $P_\tau(U) \sim U^{-2.33}$. This is slightly shallower than the earlier reported power law index of $\sim 2.5-3.0$ at ~ 1000 AU to few pc scales. The amplitude of the derived structure function is a factor of $\sim 20-60$ times higher than the extrapolated amplitude from observation of Cas A at larger scales. On the other hand, extrapolating the AU scale structure function for 3C 138 predicts the observed structure function for Cas A at the pc scale correctly. These results clearly establish that the atomic gas has significantly more structures in AU scales than expected from earlier pc scale observations. Some plausible reasons are identified and discussed here to explain these results. The observational evidence of a shallower slope and the presence of rich small scale structures may have implications for the current understanding of the interstellar turbulence.

Subject headings: ISM: atoms — ISM: general — ISM: structure — radio lines: ISM — turbulence

1. INTRODUCTION

The interstellar medium (ISM) is known to have clumpy density and velocity structures. Scale-free intensity fluctuations in a variety of tracers (e.g. H I 21 cm emission, dust emission) is detectable over a wide range of scales. This scale-free fluctuation is generally interpreted as the signature of a turbulent ISM. The evidence for small scale structures and turbulence in the atomic ISM of the Galaxy have been found through various observational techniques. Power law scaling for the velocity dispersion of the H I 21 cm emission has been observed to sub-pc scales (Roy et al. 2008). On somewhat larger scales, the intensity fluctuations in H I 21 cm emission show a scale free power spectrum (Crovisier & Dickey 1983; Green 1993; Dickey et al. 2001). The H I opacity towards Cassiopeia A and Cygnus A show fluctuations on scales ranging from 500 AU to 4 pc for the absorption in the Perseus arm, the local arm, and the Outer arm (Deshpande et al. 2000; Roy et al. 2010). Very long baseline interferometry (VLBI) observations reveal structures on scales as small as 25 AU (Dieter et al. 1976; Diamond et al. 1989; Davis et al. 1996; Faison et al. 1998; Faison & Goss 2001; Brogan et al. 2005). Deshpande et al. (1992), Frail et al. (1994), Johnston et al. (2003) and Stanimirović et al. (2010) have shown H I opacity variations on scales of $5-100$ AU from multi-epoch observations of some high velocity pulsars. Dhawan et al. (2000) have reported similar opacity variations on $40-1000$ AU scales towards the microquasar GRS $1915+105$. Observations of some other pulsars, however, do not show any opacity variations (Johnston et al. 2003; Stanimirović et al. 2003; Minter et al. 2005; Stanimirović et al. 2010), indicating that such tiny scale structures may be rare.

Small scale ISM structures are not unique to the Milky Way. The H I emission from the Large Magellanic Cloud, the Small Magellanic Cloud, several dwarf galaxies in the M81 group and a sample of dwarf and nearby spiral galaxies also show considerable small scale intensity fluctuations (Stanimirović et al. 1999; Westpfahl et al. 1999; Stanimirović & Lazarian 2001; Elmegreen et al. 2001; Begum et al. 2006; Kim et al. 2007; Dutta et al. 2009a,b).

From an observational point of view, the H I 21 cm opacity fluctuations depend on fluctuations in the density and temperature of the gas. But, for small density fluctuations, the dependence on temperature is weak (Deshpande et al. 2000). Earlier, these small fluctuations were believed to be physical structures with densities $\sim 10^4 - 10^5$ cm^{-3}. However, explaining the existence of these structures in equilibrium with orders of magnitude lower density gas in the surrounding medium, is challenging. Later, it was suggested that the fluctuations at larger spatial scales could, in projection, give rise to the observed small scale transverse fluctuations (Deshpande 2000). On the other hand, there are some direct observational evidence of ~ 3000 AU size H I structures with a density of ~ 100 cm^{-3} (Braun & Kanekar 2005; Stanimirović & Heiles 2005). Recent numerical simulations of the turbulent ISM have

---

[1] National Radio Astronomy Observatory, 1003 Lopezville Road, Socorro, NM 87801, USA

[2] Contact author's electronic address: nroy@aoc.nrao.edu (NR). NR is a Jansky Fellow of the National Radio Astronomy Observatory (NRAO). The NRAO is a facility of the National Science Foundation (NSF) operated under cooperative agreement by Associated Universities, Inc. (AUI).

[3] National Radio Astronomy Observatory, P.O. Box 2, Green Bank, WV 24944, USA

[4] National Radio Astronomy Observatory, 520 Edgemont Road, Charlottesville, VA 22903, USA

[5] Jet Propulsion Laboratory, California Institute of Technology, Pasadena, CA 91109, USA

also indicated the existence of tiny scale structures (Nagashima et al. 2003; Vázquez-Semadeni et al. 2006; Hennebelle & Audit 2007). The short evaporation timescale (~ 1 Myr) of these structures imply that they can survive if either the ambient pressure is much higher than the average ISM pressure or they are formed on a similar time-scale. In any case, their physical properties are not yet well understood.

Here we present results on tiny scale H I opacity fluctuations towards the quasar 3C 138 derived from VLBA, MERLIN and VLA data. Combining MERLIN and VLA data with VLBA data has resulted in improved sensitivity and larger spatial dynamic range to detect small optical depth fluctuations and to derive the structure function. The data analysis method is outlined in Section §2. Section §3 contains the results, and the conclusions are presented in Section §4.

2. DATA ANALYSIS

For this analysis, we have used VLBA, MERLIN and VLA data. Results from the MERLIN and VLBA observations were previously presented by Davis et al. (1996), Faison et al. (1998) and Brogan et al. (2005). The VLBA observation (Project BD0026) was carried out on September 10, 1995. The spectral resolution of this data is ~ 0.4 km s^{-1}. The MERLIN observation was carried out on October 22 and 23, 1993, and the spectral resolution in this case is ~ 0.4 km s^{-1}. The VLA A-configuration observations were carried out on September 07 and 13, 1991 (Project AS0410 and TEST). The channel width and spectral resolution in this case are ~ 0.8 and ~ 0.6 km s^{-1}, respectively. Brogan et al. (2005) reported temporal variation of H I opacity towards 3C 138 from the VLBA observations taken in 1995, but also include data from 1999 and 2002. Here, we have only included the 1995 data, since it is closest to the MERLIN and VLA observation epochs. The longest baseline was about 0.18, 1.0 and 36 Mλ (angular resolution of about 1000, 200 and 6 mas) for the VLA, MERLIN and VLBA data respectively. However, even with the combination of the VLBA, MERLIN and VLA, sufficient brightness temperature sensitivity was achieved only on angular scales larger than about 20 mas, corresponding to baselines shorter than about ~ 15 Mλ.

Data analysis was carried out using the NRAO Astronomical Image Processing System (AIPS). All the data were converted to J2000.0 epoch, and the spectral axis was regrided to a common spectral resolution of 0.4 km s^{-1}. A combined dataset was produced after first reweighting the VLBA, MERLIN and VLA data to have similar data weights (i.e. so they would contribute equally at the imaging stage). A continuum and continuum-free dataset were produced by fitting the line-free channels in the uv-plane. Self-calibration was repeatedly done on the continuum data starting with a VLBA image as the initial model, and then including the MERLIN and the VLA baselines at later stages. The self-calibration solutions obtained for the continuum data were also applied to the spectral line data cube. The final continuum image, shown in Figure (1), and the spectral line image cube were made using multiscale imaging with a 20 mas restoring beam. The structures of the continuum and line images agree with the VLBA images of Brogan et al. (2005). The spectral image cube and the continuum image were used to obtain the optical depth image cube. A 3σ cutoff was used for blanking the continuum image, and the same blanking window was applied to the spectral data to get rid of possible contribution from high noise or other low level image artifacts. The optical depth image cube was used to derive the opacity fluctuation structure function.

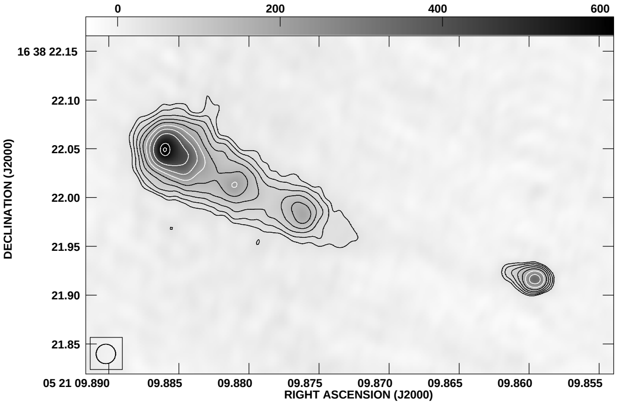

Figure 1. 1.4 GHz continuum image of 3C 138 from the combined VLBA, MERLIN and VLA data with a 20 mas restoring beam. The rms noise of the image is 12 mJy/beam. The contour levels at (1.0, 1.4, 2.0, 2.8, 4.0, 5.6, 8.0, 11.2, 16.0, 16.8) ×36 mJy/beam are overplotted on the gray scale image with linear intensity scale.

We note that the structure function amplitude of the line-free channels is more than an order of magnitude lower than the structure function amplitude of the channels with H I absorption signal. But, for the channels with H I signal, the optical depth noise is significantly higher than that of the line-free channels. Since the rms noise in the continuum image (σ_C) is significantly lower than the rms noise in line channels (σ_I), the optical depth noise can be approximated as $\sigma_\tau \approx e^\tau(\sigma_I/I_0)$, where I_0 is the continuum image flux density. Thus, for high optical depth, the noise is scaled up by a factor of e^τ. So, the optical depth noise is highly correlated with the optical depth itself. Numerical analysis shows that, as a result, the noise bias will have a similar power law dependence on all angular scales, and will scale up the structure function amplitude without changing the power law index. Moreover, the H I brightness temperature for the line channels will contribute to the system temperature, and will also increase the image noise. As a result, estimating the noise contribution from the line-free channels will underestimate the errors to the structure function due to optical depth uncertainties.

Statistical errors on the derived structure function for individual channels are estimated from the variance of the measurements within the bin, and do not account for the high optical depth measurement uncertainty. If the high opacity pixels are excluded, the effect of this uncertainty and the noise bias to the derived structure function is minimized. But in that case, the opacity image is modified by a window function, and the structure function can only be derived for about a factor of 4 smaller range of angular scales, and only $\sim 8-10$ spectral channels. Hence, first the high opacity pixels are included to derive the initial structure function. With significant noise bias, the amplitude of the structure function in this case is only an upper limit. However, one can use a larger range of

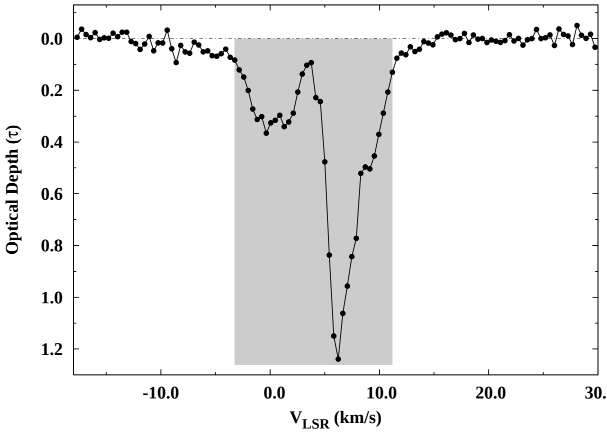

Figure 2. Integrated H I 21 cm absorption spectrum towards 3C 138 from combined VLBA, MERLIN and VLA data. The channels in the shaded region are used to derive the structure function.

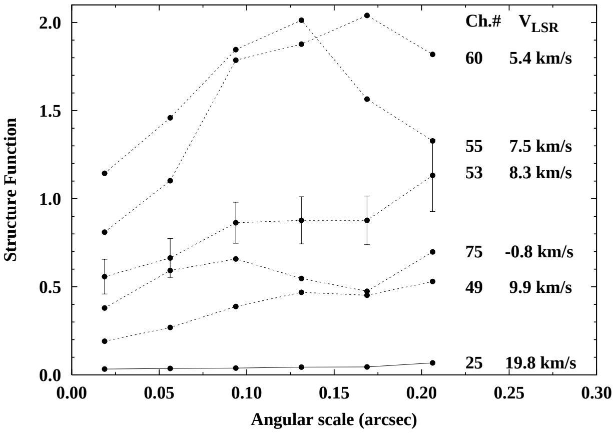

Figure 3. Structure function from a few selected channels with H I absorption (dashed line), and from one channel with no absorption (solid line). For clarity, error bars are shown for only one channel.

angular scale to fit the power law index. Then τ/σ_τ cutoff is used to minimize the noise bias and to compute the amplitude of the structure function from a limited range of angular scales. For both cases, statistical errors are estimated using the channel to channel variation of the structure function. Essentially, the opacity values in any channel may be considered as an independent realization drawn from a parent distribution of opacities with associated uncertainty. So, the channel to channel variation of the structure function will include the opacity uncertainty effect. The errors are estimated assuming that there is no spectral variation of the structure function. Thus, one can only derive an average structure function from all the spectral channels.

3. RESULTS

3C 138 is unresolved at the short baselines ($\leq 45\mathrm{k}\lambda$) of the VLA. Thus, by combining the VLBA, MERLIN and VLA data, we are able to image 3C 138 maintaining the small scale structures at the VLBA resolution, and, at the same time, restoring the total flux density observed by the VLA. The intermediate MERLIN and VLBA baselines provide a wide range of uv-coverage, allowing us to probe structures at scales ranging from about ten milliarcsec to about 0.20 arcsec. Adopting a distance to the absorbing gas of 500 pc (Faison et al. 1998), the range of angular scales translates to $5-100$ AU. The integrated H I 21 cm absorption spectrum is shown in Figure (2). The shaded region in Figure (2) indicates the channels that have adequate signal to noise in optical depth images for further analysis of small scale opacity fluctuations. We have calculated the structure function for 36 individual spectral channels, each with a velocity width of ~ 0.4 km s^{-1}, and used all the measurements together to derive the best estimate of the structure function slope and amplitude.

For quantitative study of small scale fluctuations, statistical tools like the correlation function, structure function, and power spectrum are very useful. The observed shape of these functions are expected to be related to the physical processes that gives rise to the fluctuations. The power spectrum of the opacity fluctuations $P_\tau(U)$ is the Fourier transform of the correlation function $\xi_\tau(x)$:

$$P_\tau(U) \equiv P_\tau(u,v) = \int\int \xi_\tau(l,m) e^{-2\pi i(ul+vm)} dl dm\,, \tag{1}$$

where (l,m) and (u,v) are the sky coordinate and inverse angular separation respectively. Here, $\xi_\tau(x)$ is defined as

$$\xi_\tau(x) \equiv \xi_\tau(l-l', m-m') = \langle \delta\tau(l,m)\delta\tau(l',m')\rangle \quad , \tag{2}$$

and the structure function $S_\tau(x) = [\Delta\tau(x)]^2$ is given by

$$S_\tau(x) \equiv S_\tau(l-l', m-m') = \langle [\tau(l,m) - \tau(l',m')]^2 \rangle \,. \tag{3}$$

Strictly speaking, P_τ and ξ_τ are function of $\vec{U}$ and $\vec{x}$, respectively, but we have assumed statistical isotropy for the purpose of simplification. Thus, throughout this analysis, P_τ and ξ_τ are considered to only be functions of scalar amplitude U and x, respectively. Generally, if the power spectrum is a power law of the form $P_\tau(U) = P_0 U^{-\alpha}$ with $2 < \alpha < 4$, the structure function $S_\tau(x)$ will have a power law index of $\alpha - 2$, and the rms opacity fluctuation $\Delta\tau(x)$ will have a power law index of $(\alpha-2)/2$ (Lee & Jokippii 1975; Deshpande 2000). We also note that if the density fluctuations are small (that is $\delta\rho/\langle\rho\rangle << 1$), the density fluctuation power spectrum is expected to be very similar to the opacity fluctuation power spectrum (Deshpande et al. 2000).

The derived structure function of the H I absorption towards 3C 138 for a few spectral channels are shown in Figure (3). The amplitude and the shape of the function changes from channel to channel. The structure function from one spectral channel with no H I signal is also shown in this figure for a comparison. The measured structure function for all 36 spectral channels with adequate signal to noise is shown in Figure (4). The open point symbols are structure function values without any τ/σ_τ cutoff. Clearly, below $\sim$ 10 milliarcsec, the structures are smoothed by the synthesized beam. Above $\sim$ 200 milliarcsec, the effects of the spatial window due to the shape of the continuum emission significantly modify and flatten the measured structure function. The mean and rms values of these points in each bin are shown as filled circles with error bars (with position shifted slightly to the left for clarity). The best fit power law for the ensemble (dash-dot lines in the figure) has a power law index of

0.33 ± 0.07 (3σ), which corresponds to a power spectrum with a power law index $\alpha = 2.33$.

Next, we have used a cutoff based on τ/σ_τ to minimize the noise bias and obtain a better estimate of the structure function amplitude. As mentioned earlier, with this cutoff we have a reliable estimate of the structure function only for $\sim 8 - 10$ channels and a limited range of angular scales. Here, we have used a cutoff at $\tau/\sigma_\tau = 2$ with usable range of $\sim 10 - 40$ mas for eight spectral channels. These estimates (shown as filled points joined by dotted lines in the same figure) are also consistent with a power law index of 0.33. Since $\tau/\sigma_\tau \geq 2$, the signal structure function is at least a factor of 4 higher than the noise bias case. So, the amplitude of the signal structure function is constrained to be higher than 0.8 times the observed amplitude. Unfortunately, for any higher cutoff, the flattening due to the spatial window dominates, and essentially makes it impossible to extract the true structure function. The solid line in the figure is the structure function from Deshpande (2000) extrapolated from the observed structure function power index of 0.75 in the range of $\sim 0.02 - 4.0$ pc. Clearly the observed structure function amplitude at smaller scales ($5 - 100$ AU) is $\sim 20 - 60$ times higher than the extrapolated value. In terms of rms opacity fluctuation, the observed values are a factor of $4-8$ times higher than the predicted values.

Apart from considering measurements from all the channels together for fitting, each channel is considered separately to cross-check if there is any significant channel to channel variation of the structure function. Note that the errors on the structure function derived from single channel reflect only the variance of the measurements, and do not include the effect of large optical depth uncertainties. The best fit power law amplitude and index for each channel are shown in Figure (5). Error bars for individual channels are 3σ error from the power law fit. The structure function amplitude is a factor of $2 - 5$ higher for channels with stronger absorption. This is consistent with the fact that the strong noise bias in these channels are expected to scale up the amplitude. However, we note that the average value of the power law index 0.36 ± 0.06 (3σ interval shown in dotted lines) is consistent with no channel to channel variation of the index. This best fit value of the power law index is also consistent (at better than 3σ uncertainty level) with the power law index value of 0.33 ± 0.07 we derived earlier from the ensemble of structure functions from all the channels.

Typically, the power spectra from the H I emission and absorption observations have a power law index $\alpha \sim 2.5 - 3.0$ at scales of ~ 1000 AU to a few pc (Crovisier & Dickey 1983; Green 1993; Stanimirović et al. 1999; Deshpande et al. 2000; Begum et al. 2006; Dutta et al. 2009a,b; Roy et al. 2010). For 3C 138, the derived power law index ($\alpha \sim 2.33$) for the power spectrum is slightly shallower. This flattening may arise from two reasons. Earlier it has been reported that, in the case of turbulence in a supernova remnant, a transition from 3-d to 2-d turbulence makes the power spectrum shallower (Roy et al. 2009). So, instead of homogeneous random fluctuations, anisotropic turbulence at smaller scales can result in a shallower spectrum. These fluctuations may be averaged out for large scale observations with an arcsec beam. The other plausible reason may be small scale physical processes like viscous damping. Viscous damping for incompressible magnetized turbulence can make the magnetic energy spectrum significantly less steep (Cho et al. 2002). Since, even with very small ionization fraction, H I is coupled to the Galactic magnetic field, any possible correlation of H I density with the magnetic field strength will also flatten the opacity fluctuation power spectrum. In this regard, it will be interesting to check if simulation of compressible magnetohydrodynamic turbulence including damping and anisotropy at small scales can explain these observational results quantitatively.

Our results also point out an amplitude mismatch between the observed structure function and that of the structure function extrapolated from large scale. The derived amplitude is more than an order of magnitude higher at tens of AU scale for 3C 138. The observed higher amplitude at small scales may be due to few possible reasons. First of all, for our analysis, we have used 3C 138 ($l = 187°$, $b = -11°$) as a background source, whereas Deshpande et al. (2000) used Cas A ($l = 112°$, $b = -2°$) for deriving the structure function at pc scales. These two lines of sight are widely separated, probing H I in different parts of the Galaxy, where the small scale structures may, in principle, be intrinsically different. Alternatively, it may be an effect of the uncertainty in the measurement of structure function towards Cas A, and extrapolation over a large angular scale giving rise to this mismatch. In this regard, we find that extrapolating the shallower structure function for 3C 138 to 0.5 pc scale predicts the large scale structure function amplitude within $\sim 10\%$ of the observed value for Cas A. In other words, the amplitude of the structure function at AU scales is, as expected in this second possibility, completely consistent with the observed rms opacity fluctuations at the pc scale. Finally, it is possible that there are physical mechanism(s) which modify both the amplitude and slope of the structure function at AU scales. For example density fluctuations due to intermittency may in part explain this excess of tiny scale structures. We note that, (Falgarone et al. 2009) have reported milliparsec scale extreme velocity shears, which are explained as signature of intermittency. Further observations for more lines of sight, and measurements of structure function to bridge the gap between AU and pc scales will be very helpful in distinguishing between these different possible scenarios.

4. CONCLUSIONS

We have used high resolution images of H I absorption towards 3C 138 from the combined VLA, MERLIN and VLBA data to study the small scale opacity fluctuations. The fluctuations have a power law structure function with an index of $\beta \sim 0.33 \pm 0.07$ over the scales of $\sim 5 - 100$ AU. This implies a power spectrum $P_\tau(U) \sim U^{-2.33}$, slightly shallower than the earlier reported values of $\alpha \sim 2.5 - 3.0$ from observations over larger scales. The amplitude of the structure function at the AU scale is found to be significantly higher than the extrapolated amplitude from observations of Cas A at pc scale. The observed rms opacity difference for 3C 138 is about $4 - 8$ times higher than the prediction from this extrapolation from Cas A. However, extrapolating the observed AU scale structure function for 3C 138 consis-

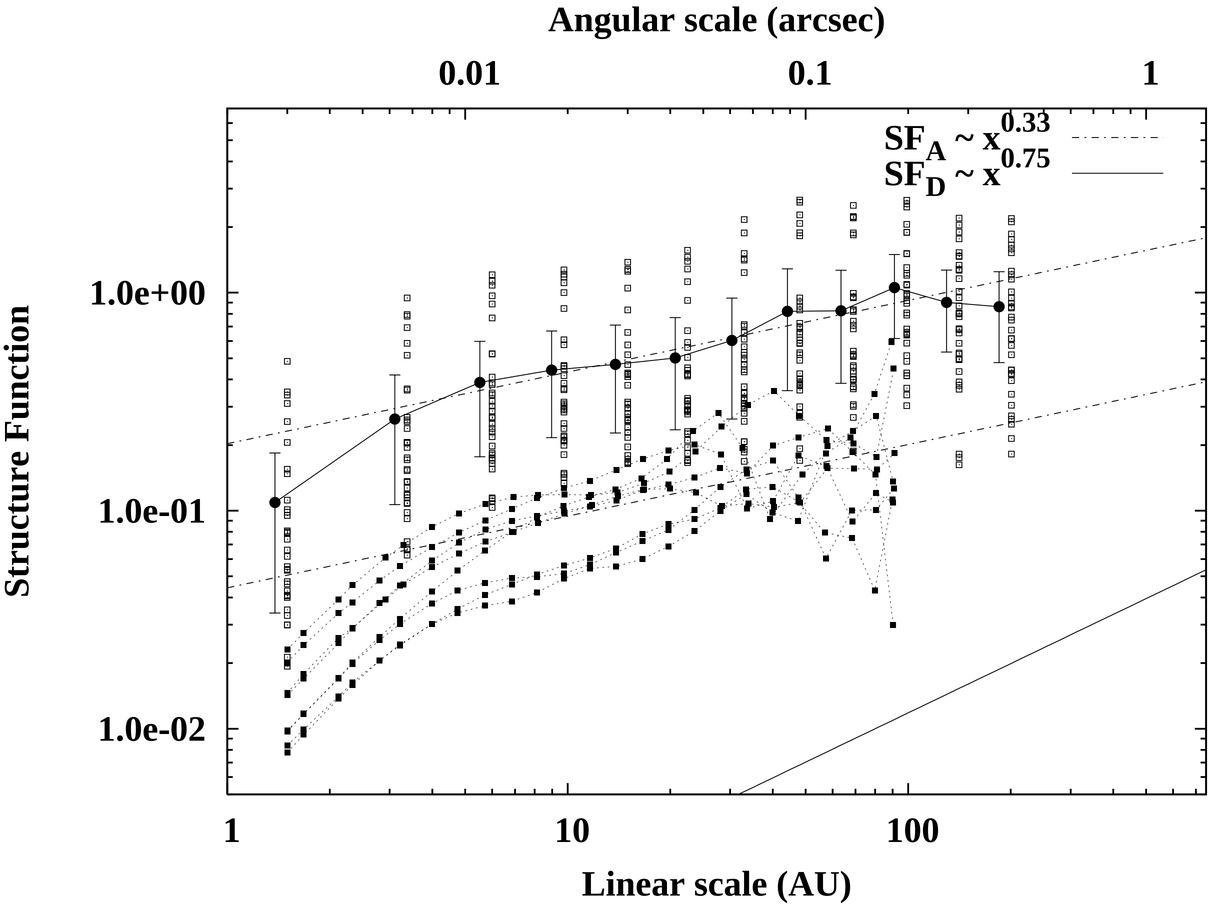

Figure 4. Measured opacity fluctuation structure function from all spectral channels with adequate signal to noise. Open squares are estimates without a τ/σ_τ cutoff. The mean and rms values in each bin are shown as filled circles with error bars (with position shifted slightly to the left for clarity). The best fit power law (shown as dash-dot lines) for the ensemble has a power law index of 0.33 ± 0.07 (3σ). The structure function derived using $\tau/\sigma_\tau = 2$ cutoff (filled squares joined by dotted lines) is also consistent with a power law index of 0.33. The solid line is the extrapolated structure function from Deshpande (2000).

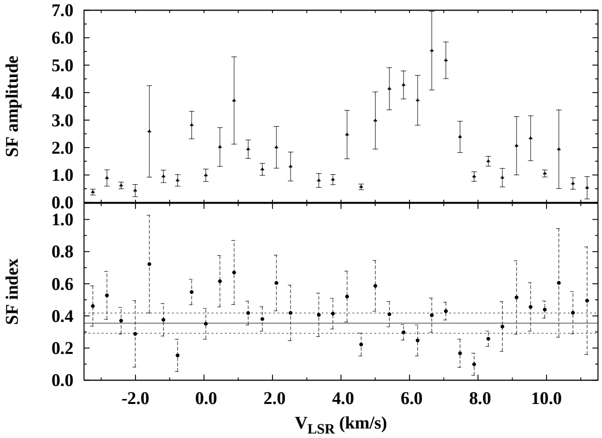

Figure 5. Channel to channel variation of the structure function. The best fit power law amplitude and index, with 3σ errors, are shown in the top and the bottom panel respectively. The average value of the power law index is 0.36 ± 0.06.

tently predicts the observed rms opacity fluctuations for Cas A at the pc scale. Physical processes like velocity intermittency, viscous damping or anisotropy of turbulence may be related to this observational indication of a shallower slope and the presence of rich structures at smaller scales. Further measurements of structure function between AU and pc scales, and detailed numerical simulations to quantitatively verify these results can improve the understanding of the interstellar turbulence.

We thank the anonymous referee for many useful comments which prompted us into improving this paper substantially. We also thank John Scalo, Deputy Editor of ApJ Letters, for useful suggestions. We are grateful to Jayaram N. Chengalur, Avinash A. Deshpande, Prasun Dutta and Snezana Stanimirović for helpful discussions and useful comments on an earlier version of this manuscript. Part of this research was carried out at the Jet Propulsion Laboratory, California Institute of Technology, under a contract with the National Aeronautics and Space Administration.

REFERENCES

Begum A., Chengalur J. N., Bhardwaj S., 2006, MNRAS, 372, L33
Braun R., Kanekar N., 2005, A&A, 436, L53
Brogan C. L., Zauderer B. A., Lazio T. J., Goss W. M., DePree C. G., Faison M. D., 2005, AJ, 130, 698
Cho J., Lazarian A., Vishniac E. T., 2002, ApJ, 566, L49

Crovisier J., Dickey J. M., 1983, A&A, 122, 282
Davis R. J., Diamond P. J., Goss W. M., 1996, MNRAS, 283, 1105
Deshpande A. A., McCulloch P. M., Radhakrishnan V., Anantharamaiah K. R., 1992, MNRAS, 258, 19P
Deshpande A. A., 2000, MNRAS, 317, 199
Deshpande A. A., Dwarakanath K. S., Goss W. M., 2000, ApJ, 543, 227
Dhawan V., Goss W. M., Rodríguez L. F., 2000, ApJ, 540, 863
Diamond P. J., Goss W. M., Romney J. D., Booth R. S., Kalberla P. M. W., Mebold U., 1989, ApJ, 347, 302
Dickey J. M., McClure-Griffiths N. M., Stanimirović S., Gaensler B. M., Green A. J., 2001, ApJ, 561, 264
Dieter N. H., Welch W. J., Romney J. D., 1976, ApJ, 206, L113
Dutta P., Begum A., Bharadwaj S., Chengalur J. N., 2009a, MNRAS, 397, L60
Dutta P., Begum A., Bharadwaj S., Chengalur J. N., 2009b, MNRAS, 398, 887
Elmegreen B. G., Kim S., Staveley-Smith L., 2001, ApJ, 548, 749
Faison M. D., Goss W. M., Diamond P. J., Taylor G. B., 1998, AJ, 116, 2916
Faison M. D., Goss W. M., 2001, AJ, 121, 2706
Falgarone E., Pety J., Hily-Blant P., 2009, A&A, 507, 355
Frail D. A., Weisberg J. M., Cordes J. M., Mathers C., 1994, ApJ, 436, 144
Green D. A., 1993, MNRAS, 262, 327
Hennebelle P., Audit E., 2007, A&A, 465, 431
Johnston S., Koribalski B., Wilson W., Walker M., 2003, MNRAS, 341, 941
Kim S. et al., 2007, ApJS, 171, 419
Lee L. C., Jokippii J. R., 1975, ApJ, 196, 695
Minter A. H., Balser D. S., Kartaltepe J. S., 2005, ApJ, 631, 376
Nagashima M., Inutsuka S.-I., Koyama H., 2006, ApJ, 652, 41
Roy N., Peedikakkandy L., Chengalur J. N., 2008, MNRAS, 387, L18
Roy N., Bharadwaj S., Dutta P., Chengalur J. N., 2009, MNRAS, 393, L26
Roy N., Chengalur J. N., Dutta P., Bharadwaj S., 2010, MNRAS, 404, L45
Stanimirović S., Staveley-Smith L., Dickey J. M., Sault R. J., Snowden S. L., 1999, MNRAS, 302, 417
Stanimirović S., Lazarian A., 2001, ApJ, 551, L53
Stanimirović S., Weisberg J. M., Hedden A., Devine K. E., Green J. T., 2003, ApJ, 598, L23
Stanimirović S., Heiles C., 2005, ApJ, 631, 371
Stanimirović S., Weisberg J. M., Pei Z., Tuttle K., Green J. T., 2010, ApJ, 720, 415
Vázquez-Semadeni E., Ryu D., Passot T., González R., Gazol A., 2006, ApJ, 643, 245
Westpfahl D. J., Coleman P. H., Alexander J., Tongue T., 1999, AJ, 117, 868